International Communications in Heat and Mass Transfer 122 (2021) 105177

Contents lists available at ScienceDirect

International Communications in Heat and Mass Transfer

journal homepage: www.elsevier.com/locate/ichmt

Transportation of hybrid nanoparticles in forced convective Darcy-Forchheimer flow by a rotating disk

M. Ijaz Khan

Department of Mathematics and Statistics, Riphah International University I-14, Islambad 44000, Pakistan

ARTICLE INFO

Keywords:
Hybrid nanofluid
Entropy generation
Mixed convection
Darcy-Forchheimer model
Velocity and thermal slips
Non-linear thermal radiation

ABSTRACT

This research article explores the effect of entropy generation through a non-linear radiative flow of viscous fluid of hybrid nanoparticles over a stretchable rotating disk. Mixed convection and slip conditions i-e velocities and thermal are examined. The examination is accomplished in aluminum oxide (Al_2O_3)-water and copper (Cu)-water nanofluids. Similarity transformations are utilized to reduce the governing problem into the nonlinear ordinary differential equations. Flow in the permeable medium is analyzed by assuming the Darcy-Forchheimer model. The impact of various parameters consisting of mixed convection parameter, porosity parameter, velocities as well as thermal slips parameters, stretching parameter, non-linear radiation parameter, and Reynolds number on radial velocity profile, tangential velocity profile and temperature profile are studied. Also, entropy generation and heat transfer rates have been analyzed in view of different parameters in the current study. The mathematical formulation is numerically solved by the bvp4c techniques

1. Introduction

Carrying of heat energy has significant applications in industrial engineering. The efficacy of a thermal cooling procedure proportional to the amount of heat transfer rate. An increment of cooling or heating processes affects the many factors such as storage of energy, Colorado cooler, etc. Consequently, an increment in heat transfer becomes a major concern about thermal processes. There are many techniques applied for heat transportation. These techniques consisting of cooling fins, jet impingement, vibrations, etc. In the recent study of heat transfer rate the application of nano-sized materials in a base fluid which is comparatively better then, the above-revealed techniques have been used. Numerous experimental and theoretical research work has been published by examined the thermophysical significance of nanofluids. The heat transfer rate depends upon the thermal conductivity of nanofluids. The thermal conductivity of nanofluids is a function of volume fraction of nanoparticles and the thermal conductivity of the base fluid (water) and solid nano-particles. Maxwell [1] is the first one who gave the model in the context of thermal conductivity. The heat transfer mechanism for nanofluids deliberated through the thermal conductivity was given by Xue [2]. Newly, researchers introduce different kinds of nano-particles called hybrid nano-particles in their research. A hybrid nanofluid is made of two different classes of nanoparticles dissolving in a base fluid. Wang et al. [3] investigate the thermal conductivity of copper oxide (CuO) and aluminum oxide (Al_2O_3) based hybrid nanofluids is greater than the nanofluids.

Fluid flow subject to the rotating disk is a classical problem, which has many applications in various technical procedures such as lubrication, disk drives, preparation of crystal, etc. Kármán [4] was solved this problem by using the transformations known as Von Kármán transformation in 1921. Cochran [5] modified the same problem for better results. Benston [6] gave the solution for the case of the time-dependent problem.

Applications of mixed convective flow occur in various fields of engineering and technology e.g. solar thermal electricity, cooling processes of nuclear reactors, flow with different temperatures, etc. The buoyancy force is the more significant characteristic of mixed convection by changeable temperature and density. Mixed convective flow characterized into free convective or forced convective flow by bouncy parameter $\left(\frac{Gr}{\mathrm{Re}^2}\right)$ whereas (Gr) (represent the free convection) and (Re) (represent the forced convection). Natural convection is the prevalent type of heat transportation when buoyancy→0 and for the forced convection when buoyancy→∞ stated in Refs. [7–15].

Thermal radiation denotes the transfer of thermal energy into electromagnetic energy. The properties of thermal radiations are consist of surface, its absorptance, emissive power, and temperature which described by Kirchhoff's law. Transportation of heat due to the effect of

E-mail address: ijazfmg_khan@yahoo.com.

https://doi.org/10.1016/j.icheatmasstransfer.2021.105177

Available online 8 February 2021

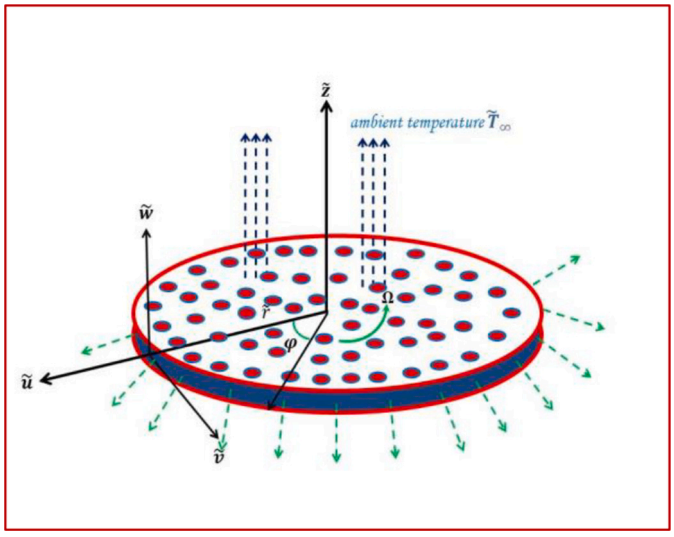

Fig. 1. Schematic flow diagram.

thermal radiation has various applications in jets, gas turbines, space crafts, satellites, rockets etc. Number of researchers have been explored the impact of thermal radiation by assuming the linear Rosseland Approximation, which is applicable on only small temperature difference within the flow. Currently, many researchers discuss the impact of nonlinear radiative heat transfer considering the nonlinear Rosseland Approximation which is applicable for both ambient and low temperatures. Farooq et al. [16] investigated the effects of nonlinear radiation on the viscoelastic nanofluids. Few research papers on nonlinear radiations are obtainable in the Refs. [17–25]

Currently, to improve the performance of fluids in energy consumption, consider some effective systems to decrease the amount of insufficient energy, which becomes the cause of the irreversibility of the fluid system. The role of entropy optimization is considered in various thermal mechanisms, such as refrigerators, power plants, combustion engines, etc. Bejan [26,27] initially gave the idea of entropy optimization. Arikoglu et al. [28] investigate the entropy generation due to a rotating disk with slip effects. Further research on entropy analysis mentioned in Refs. [29–37].

Our attention on the current study to analyze the entropy optimization in flow of Al_2O_3-water and Cu-water based hybrid nanofluids over a stretchable rotating disk subject to nonlinear thermal radiation and slip conditions. Also obtain graphical results for skin friction coefficient and Nusselt number. The entropy generation rate depends upon the following irreversibilities (i) Thermal irreversibility, (ii) porosity irreversibility and (iii) fluid friction irreversibility. Governing nonlinear equations are solved by bvp4c method.

2. Problem description

Contemplate steady non-linear radiative, mixed convective flow of hybrid-nanofluids over premeable rotating disk along with angular velocity Ω. on z-axis. The disk is stretching circumferentially with the rate a_1. Let us consider a non-rotary cylindrical coordinates $(\tilde{r},\varphi,\tilde{z})$ in such a way that disk is placed at $\tilde{z}=0$ and hybrid-nanofluid reserved at $\tilde{z}>0$ (see Fig. 1). Where $(\tilde{u},\tilde{v},\tilde{w})$ denote the components of velocities along $(\tilde{r},\varphi,\tilde{z})$ Furthermore flow is analyzed under the consideration of velocity and thermal slip conditions on boundaries. $\tilde{T}_{\tilde{w}}$ is the temperature of rotating disk at the surface while $\tilde{T}_\infty$ is the ambient temperature away from the surface of the disk. According to the above suppositions, the mathematical form of the current flow problem is:

$$\frac{\partial\tilde{u}}{\partial\tilde{r}}+\frac{\tilde{u}}{\tilde{r}}+\frac{\partial\tilde{w}}{\partial\tilde{z}}=0, \tag{1}$$

$$\tilde{u}\frac{\partial\tilde{u}}{\partial\tilde{r}}-\frac{\tilde{v}^2}{\tilde{r}}+\tilde{w}\frac{\partial\tilde{u}}{\partial\tilde{z}}=\nu_{hnf}\left(\frac{\partial^2\tilde{u}}{\partial\tilde{z}^2}+\frac{1}{\tilde{r}}\frac{\partial\tilde{u}}{\partial\tilde{r}}-\frac{\tilde{u}}{\tilde{r}^2}\right)-\frac{\nu_{hnf}}{K^*}\tilde{u}-Fu^2+\frac{g(\rho\tilde{\beta})_{hnf}}{\rho_{hnf}}\left(\tilde{T}-\tilde{T}_\infty\right)=0, \tag{2}$$

$$\tilde{u}\frac{\partial\tilde{v}}{\partial\tilde{r}}+\frac{\tilde{u}\tilde{v}}{\tilde{r}}+\tilde{w}\frac{\partial\tilde{v}}{\partial\tilde{z}}=\nu_{hnf}\left(\frac{\partial^2\tilde{v}}{\partial\tilde{r}^2}+\frac{1}{\tilde{r}}\frac{\partial\tilde{v}}{\partial\tilde{r}}+\frac{\partial^2\tilde{v}}{\partial\tilde{z}^2}-\frac{\tilde{v}}{\tilde{r}^2}\right)-\frac{\nu_{hnf}}{K^*}\tilde{v}-Fv^2, \tag{3}$$

$$\tilde{u}\frac{\partial\tilde{w}}{\partial\tilde{r}}+\tilde{w}\frac{\partial\tilde{w}}{\partial\tilde{z}}=\nu_{hnf}\left(\frac{\partial^2\tilde{w}}{\partial\tilde{r}^2}+\frac{1}{\tilde{r}}\frac{\partial\tilde{w}}{\partial\tilde{r}}+\frac{\partial^2\tilde{w}}{\partial\tilde{z}^2}-\frac{\tilde{v}}{\tilde{r}^2}\right)-\frac{\nu_{hnf}}{K^*}\tilde{w}-F\tilde{w}^2, \tag{4}$$

$$\tilde{u}\frac{\partial\tilde{T}}{\partial\tilde{r}}+\tilde{w}\frac{\partial\tilde{T}}{\partial\tilde{z}}=\alpha_{hnf}\left(\frac{\partial^2\tilde{T}}{\partial\tilde{r}^2}+\frac{1}{\tilde{r}}\frac{\partial\tilde{T}}{\partial\tilde{r}}+\frac{\partial^2\tilde{w}}{\partial\tilde{z}^2}\right)-\frac{1}{(\rho c_p)_{hnf}}\frac{\partial q_{\tilde{r}}}{\partial\tilde{z}}+\frac{\mu_{hnf}}{(\rho c_p)_{hnf}}\left[\left(\frac{\partial\tilde{u}}{\partial\tilde{z}}\right)^2+\left(\frac{\partial\tilde{v}}{\partial\tilde{z}}\right)^2\right]\Bigg\}, \tag{5}$$

with

$$\left.\begin{aligned}\tilde{u}=a_1\tilde{r}+L_1\frac{\partial\tilde{u}}{\partial\tilde{z}},\quad \tilde{v}=r\Omega+L_2\frac{\partial\tilde{v}}{\partial\tilde{z}},\quad \tilde{w}=0,\quad \tilde{T}_{\tilde{w}}=\tilde{T}+L_3\frac{\partial\tilde{T}}{\partial\tilde{z}},\quad \text{at } \tilde{z}=0,\\ \tilde{u}\to0,\quad \tilde{v}\to0,\quad \tilde{T}\to\tilde{T}_\infty,\quad \text{as } \tilde{z}\to\infty,\end{aligned}\right\} \tag{6}$$

where $\tilde{r},\varphi,\tilde{z}$ denotes cylindrical coordinates, $\tilde{u},\tilde{v},\tilde{w}$ velocities components, ν_{hnf} kinematic viscosity, K^* permeability of porous medium, $F=\frac{C_b}{K^{*\frac{1}{2}}}$ non-uniform inertia coefficient of porous medium, C_b drag coefficient, $\tilde{\beta}$ thermal expansion co-efficient, g gravity, ρ_{hnf} density, $\tilde{T}$ temperature, a_1 stretching rate, $\tilde{T}_\infty$ ambient temperature, α_{hnf} thermal diffusivity, $q_{\tilde{r}}$ radiative heat flux, $(c_p)_{hnf}$ specific heat capacity, μ_{hnf} dynamic viscosity, L_1,L_2 velocities slips along $\tilde{u},\tilde{v}$ directions respectively, Ω angular frequency, $\tilde{T}_{\tilde{w}}$ wall temperature and L_3 thermal slip. Note that *hnf* stands for the hybrid nanofluid.

Rosseland [25] was given that radiative heat flux expression is defined as

$$q_{\tilde{r}}=-\frac{4\tilde{\sigma}}{3\tilde{k}}\frac{\partial\tilde{T}^4}{\partial\tilde{z}}=-\frac{16\tilde{\sigma}T^3}{3\tilde{k}}\frac{\partial\tilde{T}}{\partial\tilde{z}}, \tag{7}$$

where $\tilde{k}$ and $\tilde{\sigma}$ indicate respectively the mean absorption coefficient and Stefan-Boltzmann constant. By the use of Rosseland formula it can be linearized about ambient temperature. This means that the equation (5)

$$\tilde{u}\frac{\partial\tilde{T}}{\partial\tilde{r}}+\tilde{w}\frac{\partial\tilde{T}}{\partial\tilde{z}}=\left(\alpha_{hnf}+\frac{16\tilde{\sigma}T_\infty^3}{3(\rho c_p)_{hnf}\tilde{k}}\right)\frac{\partial^2\tilde{T}}{\partial^2\tilde{z}}+\alpha_{hnf}\left(\frac{1}{\tilde{r}}\frac{\partial\tilde{T}}{\partial\tilde{r}}+\frac{\partial^2\tilde{w}}{\partial\tilde{z}^2}\right)+\frac{\mu_{hnf}}{(\rho c_p)_{hnf}}\left[\left(\frac{\partial\tilde{u}}{\partial\tilde{z}}\right)^2+\left(\frac{\partial\tilde{v}}{\partial\tilde{z}}\right)^2\right]\Bigg\}, \tag{8}$$

can be expressed as

Thermo-physical attributes of hybrid-nanofluids

$$\rho_{nf} = (1-\phi)_{bf} + \phi\rho_s, \tag{9}$$

$$\rho_{hnf} = \phi_{Al}\rho_{Al} + \phi_{Cu}\rho_{Cu} + (1-\phi_{Al}-\phi_{Cu})\rho_{bf}, \tag{10}$$

$$(\rho c_p)_{hnf} = \phi_{Al}\rho_{Al} + \phi_{Cu}\rho_{Cu} + (1-\phi_{Al}-\phi_{Cu})(\rho c_p)_{bf} + \phi_{Al}(\rho c_p)_{Al} + \phi_{Cu}(\rho c_p)_{Cu}, \tag{11}$$

$$k_{nf} = \frac{(k_s+2_{bf}) - 2\phi(k_{bf}-k_s)}{(k_s+2_{bf}) + 2\phi(k_{bf}-k_s)}k_{bf}, \tag{12}$$

$$\frac{k_{hnf}}{k_{bf}} = \frac{\frac{\phi_{Al}\rho_{Al}+\phi_{Cu}\rho_{Cu}}{\phi_{Al}+\phi_{Cu}} + 2k_{bf} + 2(\phi_{Al}k_{Al}+\phi_{Cu}k_{Cu}) - 2(\phi_{Al}+\phi_{Cu})k_{bf}}{\frac{\phi_{Al}\rho_{Al}+\phi_{Cu}\rho_{Cu}}{\phi_{Al}+\phi_{Cu}} + 2k_{bf} - (\phi_{Al}k_{Al}+\phi_{Cu}k_{Cu}) - (\phi_{Al}+\phi_{Cu})k_{bf}}, \tag{13}$$

$$\mu_{nf} = \frac{\mu_{bf}}{(1-\phi)^{2.5}}, \tag{14}$$

$$\nu_{hnf} = \frac{\mu_{hnf}}{\rho_{hnf}}, \tag{15}$$

$$\mu_{hnf} = \frac{\mu_{bf}}{(1-\phi_{Al}-\phi_{Cu})^{2.5}}, \tag{16}$$

$$\alpha_{hnf} = \frac{k_{hnf}}{(\rho c_p)_{hnf}}. \tag{17}$$

Note that (ρ_{hnf}) highlights the density, $(\rho c_p)_{hnf}$ specific heat capacity, (k_{hnf}) thermal conductivity, (μ_{hnf}) dynamic viscosity, (ν_{hnf}) kinematic viscosity and (α_{hnf}) is the thermal diffusivity.

Letting

$$\eta = \left(\frac{2\Omega}{\nu_f}\right)^{\frac{1}{2}}\widetilde{z},\ \widetilde{u} = \gamma\Omega f'(\eta),\ \widetilde{v} = \gamma\Omega g(\eta),\ \widetilde{w} = -\left(2\Omega\nu_f\right)^{\frac{1}{2}}f(\eta),\ \theta(\eta) = \frac{\widetilde{T}-\widetilde{T}_\infty}{\widetilde{T}_\omega-\widetilde{T}_\infty}. \tag{18}$$

By the use of $\widetilde{T} = \widetilde{T}_\infty\left(1+\theta\left(\theta_{\widetilde{w}}-1\right)\right)$, whereas $\theta_{\widetilde{w}}\left(=\frac{\widetilde{T}_w}{\widetilde{T}_\infty}\right)$ is the temperature ratio parameter with the property $\left(\widetilde{T}_\infty < \widetilde{T}_{\widetilde{w}}\right)$.

Making the use of Eq. (18), the Eq. (1) is automatically fulfilled and the remaining equations are

$$B_1(2f''' - \lambda f') + 2ff'' - (1+F_r)f'^2 + g^2 + \lambda^* B_2\theta = 0, \tag{19}$$

$$B_1(2g'' - \lambda g) + 2fg' - 2f'g - F_r g^2 = 0, \tag{20}$$

$$\frac{1}{Pr}\left(\frac{k_{hnf}}{k_{bf}}\right)\theta'' + \frac{R_d}{Pr}(\theta(\theta_\omega-1)+1)^2\left(3\theta'^2(\theta_\omega-1) + ((\theta_\omega-1)+1)\theta\theta''\right) + B_3 f\theta' = 0, \tag{21}$$

where B_1, B_2, B_3 are addressed as

$$B_1 = \frac{1}{(1-\phi_{Al}-\phi_{Cu})^{2.5}\left(1-\phi_{Al}-\phi_{Cu}+\frac{\rho_{Al}}{\rho_{bf}}\phi_{Al}+\frac{\rho_{Cu}}{\rho_{bf}}\phi_{Cu}\right)}, \tag{22}$$

$$B_2 = \frac{(1-\phi_{Al}-\phi_{Cu})^{2.5}\left(1-\phi_{Al}-\phi_{Cu}+\frac{(\rho\beta)_{Al}}{(\rho\beta)_{bf}}\phi_{Al}+\frac{(\rho\beta)_{Cu}}{(\rho\beta)_{bf}}\phi_{Cu}\right)}{\left(1-\phi_{Al}-\phi_{Cu}+\frac{\rho_{Al}}{\rho_{bf}}\phi_{Al}+\frac{\rho_{Cu}}{\rho_{bf}}\phi_{Cu}\right)}, \tag{23}$$

$$B_3 = \left(1-\phi_{Al}-\phi_{Cu}+\frac{(\rho c_p)_{Al}}{(\rho c_p)_{bf}}\phi_{Al}+\frac{(\rho c_p)_{Cu}}{(\rho c_p)_{bf}}\phi_{Cu}\right), \tag{24}$$

with

$$\left.\begin{array}{c} f(\eta)=0, f'(\eta)-\beta f''(\eta)=A_1, g(\eta)-\gamma g'(\eta)=1, \theta(\eta)-\gamma^*\theta'(\eta)=1, \text{at}\,\eta=0, \\ f'(\eta)\to 0,\ g(\eta)\to 0,\ \theta(\eta)\to 0,\ \text{as}\,\eta\to\infty, \end{array}\right\} \tag{25}$$

where prime highlights derivative with respect to η, $\lambda^*\left(=\frac{(g\beta)_{bf}\left(\widetilde{T}_w-\widetilde{T}_\infty\right)}{r\Omega^2}\right)$ the mixed convective variable, $F_r\left(\frac{C_b}{K^{1/2}}\right)$ the Darcy parameter, $\lambda\left(=\frac{\nu_{bf}}{K^*\Omega}\right)$ the porosity parameter, $A_1\left(=\frac{a_1}{\Omega}\right)$ the stretching parameter, $Re\left(=\frac{\Omega r^2}{\nu_{bf}}\right)$ the Reynolds number, $\theta_{\widetilde{w}}\left(=\frac{\widetilde{T}_\omega}{\widetilde{T}_\infty}\right)$ the temperature ratio, $R_d\left(=\frac{16}{3}\frac{\widetilde{\sigma}\widetilde{T}_\infty}{\widetilde{k}k_{bf}}\right)$ the radiation parameter, $\beta\left(=\left(\frac{\Omega}{\nu_{bf}}\right)^{1/2}L_1\right)$ the radial velocity slip parameter, $Pr\left(=\frac{\nu_{bf}}{\alpha_{bf}}\right)$ the Prandtl number, $\gamma\left(=\left(\frac{b}{\nu_{bf}}\right)^{1/2}L_2\right)$ the tangential velocity slip parameter, $\gamma^*\left(=\left(\frac{b}{\nu_{bf}}\right)^{1/2}L_3\right)$ the thermal slip parameter denotes the and $Br =$ Pr . Ec denotes the Brinkman number.

3. Entropy generation

In the late 19th century the concept of entropy generation was introduced by Ludwig Boltzmann. Mathematical form of entropy is given as

$$N_G = \frac{k_{bf}}{\widetilde{T}_\infty}\left(\frac{k_{hnf}}{k_{bf}}+\frac{16}{3}\frac{\widetilde{\sigma}\widetilde{T}^3}{\widetilde{k}k_{bf}}\right)\left(\frac{\partial\widetilde{T}}{\partial\widetilde{z}}\right)^2 + \frac{\mu_{hnf}}{K^*\widetilde{T}_\infty}(\widetilde{u}^2+\widetilde{v}^2) + \frac{\mu_{hnf}}{\widetilde{T}_\infty}\left[\begin{array}{l} 2\left(\frac{\partial\widetilde{u}}{\partial\widetilde{r}}\right)^2 + \frac{2u^2}{\widetilde{r}^2} + \left(\frac{\partial\widetilde{v}}{\partial\widetilde{z}}\right)^2 \\ +\left(\frac{\partial\widetilde{u}}{\partial\widetilde{z}}\right)^2 + 2\left(\frac{\partial\widetilde{w}}{\partial\widetilde{z}}\right)^2 + \left(\widetilde{r}\frac{\partial}{\partial\widetilde{r}}\left(\frac{\widetilde{v}}{\widetilde{r}}\right)\right)^2 \end{array}\right], \tag{26}$$

and the dimensionless form is

$$\left.\begin{array}{c} N_G = 2\left(\frac{k_{hnf}}{K_{bf}}+R_d((\theta_\omega-1)+1)^3\right)\alpha_1\theta'^2 + \frac{\lambda Br}{(1-\phi_{Al}-\phi_{Cu})^{2.5}}\left(f'^2+g^2\right) \\ +\frac{Br}{(1-\phi_{Al}-\phi_{Cu})^{2.5}Re}\left(12f'^2+Re\left(g'^2+f''^2\right)\right), \end{array}\right\} \tag{27}$$

where $Br\left(=\frac{\mu_{bf}\Omega^2\widetilde{r}^2}{K_{bf}\Delta\widetilde{T}}\right)$ signifies the Brinkman number.

4. Engineering quantities

4.1. Skin friction coefficient

The mathematical form of local skin frictions co-efficient is

$$C_f = \frac{\tau_\omega}{\rho_{hnf}(r\Omega)^2}, \tag{28}$$

Table 1
Thermo-physical attributes of Aluminum Oxide, Copper and Water.

Physical properties	Nanoparticles		Pure water
	Aluminum oxide (Al_2O_3)	Copper (Cu)	
$\rho(kg/m^3)$	3970	8933	997.1
$k(\widetilde{w}/mK)$	40	401	0.613
$c_p(j/kgK$	765	385	4179

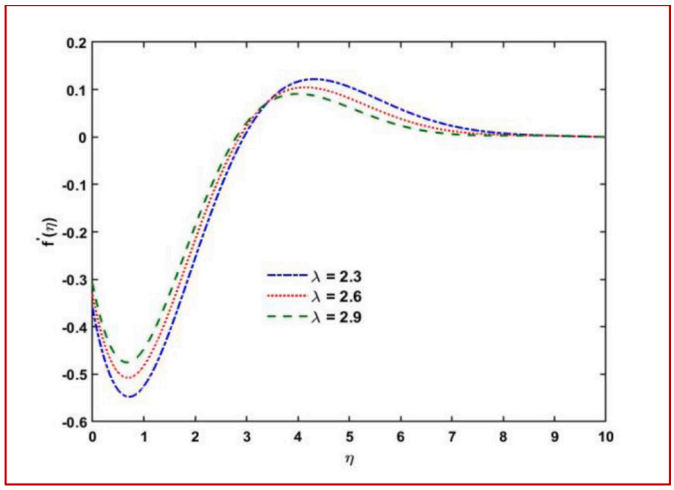

Fig. 2. $f'(\eta)$ *versus* λ.

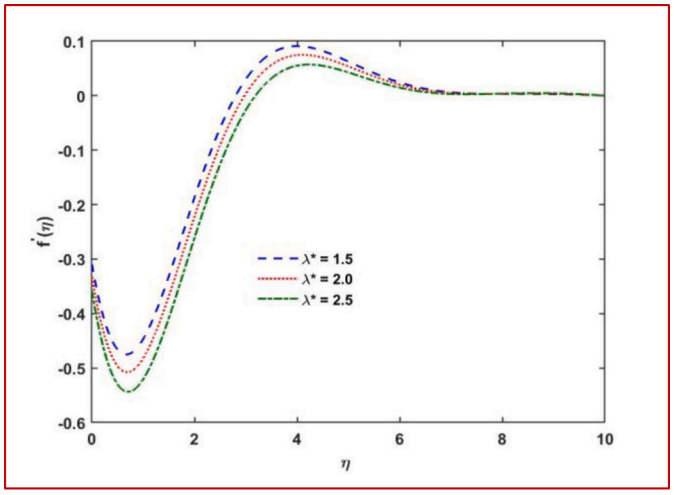

Fig. 3. $f'(\eta)$ *versus* λ^*.

where τ_ω is the total shear stress is defined as

$$\tau_\omega = \sqrt{\tau_{\omega r} + \tau_{\omega\theta}}, \tag{29}$$

where $(\tau_{\omega r}, \tau_{\omega\theta})$ are the shear stresses and mathematically deliberated as

$$\left.\begin{aligned} \tau_{\omega r} &= \left(\mu_{hnf}\frac{\partial \widetilde{u}}{\partial \widetilde{z}}\right)_{\widetilde{z}=0}, \\ \tau_{\omega\theta} &= \left(\mu_{hnf}\frac{\partial \widetilde{v}}{\partial \widetilde{z}}\right)_{\widetilde{z}=0}, \end{aligned}\right\} \tag{30}$$

Non-dimensional form of skin friction co-efficient is given as

$$C_f \mathrm{Re}^{1/2} = \sqrt{2}B_1\left(f''(0)^2 + g'(0)^2\right)^{1/2}. \tag{31}$$

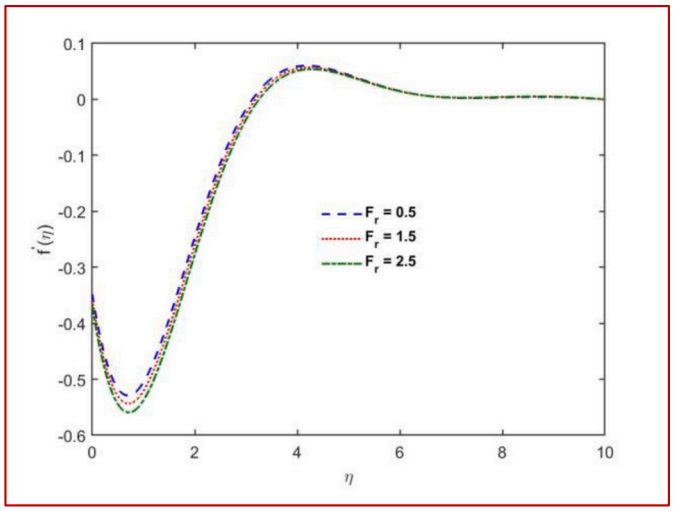

Fig. 4. $f'(\eta)$ *versus* F_r.

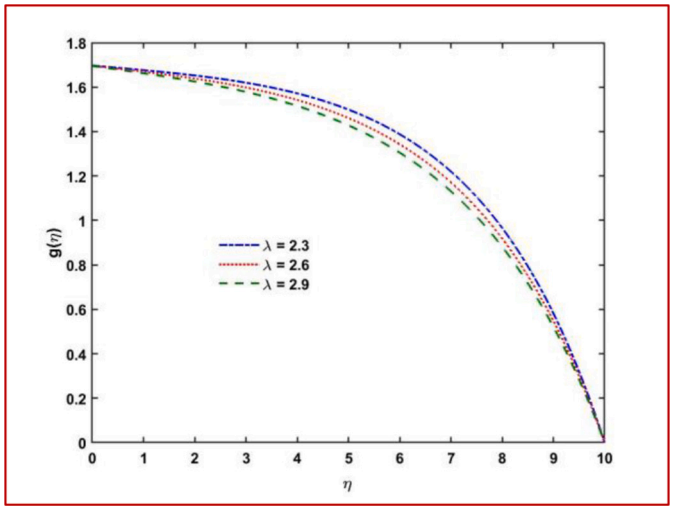

Fig. 5. $g(\eta)$ *versus* λ.

4.2. Heat transfer rate

Mathematically, we have

$$N_u = \frac{\widetilde{r}q_\omega}{k_{hnf}\left(\widetilde{T}_{\widetilde{w}} - \widetilde{T}_\infty\right)}, \tag{32}$$

where $q_{\widetilde{w}}$ is defined as

$$q_\omega = -\left(k_{hnf}\frac{\partial \widetilde{T}}{\partial \widetilde{z}}\right)_{\widetilde{z}=0} + \left(q_{\widetilde{r}}\right)_{\widetilde{z}=0}, \tag{33}$$

Finally, we have

$$Nu\mathrm{Re}^{-1/2} = -\sqrt{2}\left(\left(\frac{k_{hnf}}{k_{bf}}\right) + R_d\left(1+\theta(0)\left(\theta_{\widetilde{w}}-1\right)\right)^3\right)\theta'(0) \tag{34}$$

5. Graphical analysis

The nonlinear thermal radiative flow of hybrid nanofluid on a preamble rotating disk are investigated through slip conditions on boundaries. Entropy generation and heat transfer effects are discussed. The impacts of various dynamic parameters, consisting mixed convection

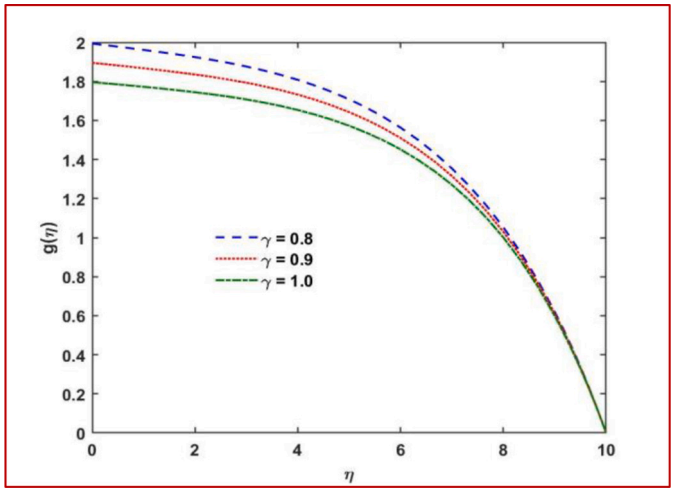

Fig. 6. $g(\eta)$ *versus* γ.

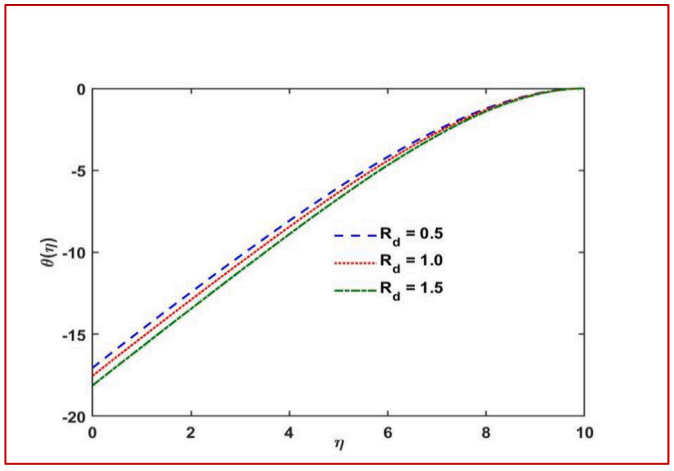

Fig. 7. $\theta(\eta)$ *versus* R_d.

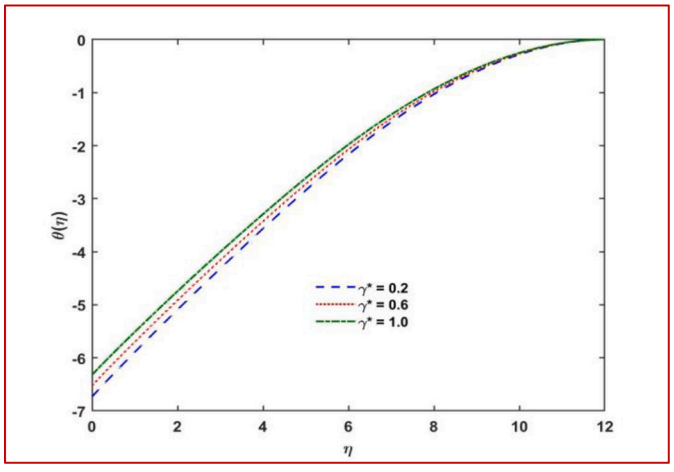

Fig. 8. $\theta(\eta)$ *versus* γ^*.

parameter (λ^*), porosity parameter (λ), velocities as well as thermal slips parameters (β, γ, γ^*), stretching parameter (A_1), Reynolds number (Re), Brinkman number (Br), and radiation parameter (R_d), through the entropy generation, Nusselt number, radial and tangential velocity fields and temperature profiles. We have discussed the thermo-physical

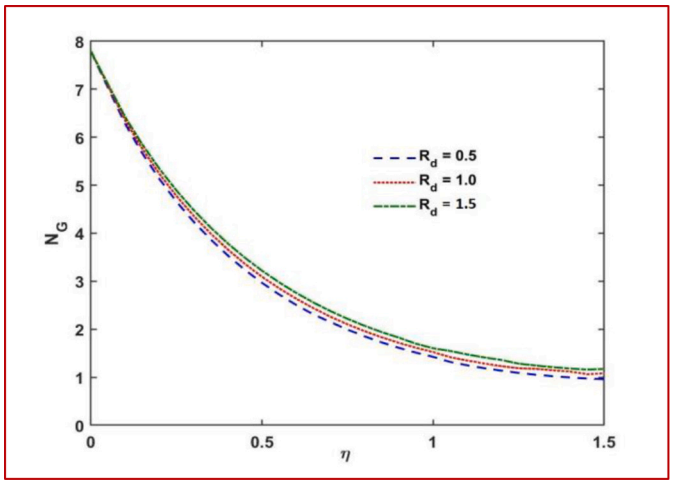

Fig. 9. $N_G(\eta)$ *versus* R_d.

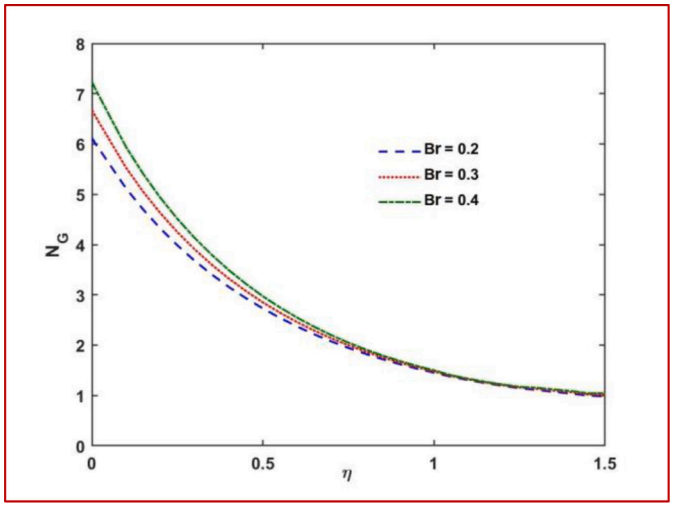

Fig. 10. $N_G(\eta)$ *versus* Br.

properties of hybrid- nanofluids in Table 1. Also, we assumed a distinct volume fraction $\phi_{Cu} = 0.05$ and $\phi_{Al} = 0.05$ of Copper and silver based nanoparticles respectively. Fig. 2 portrays the impact of porosity

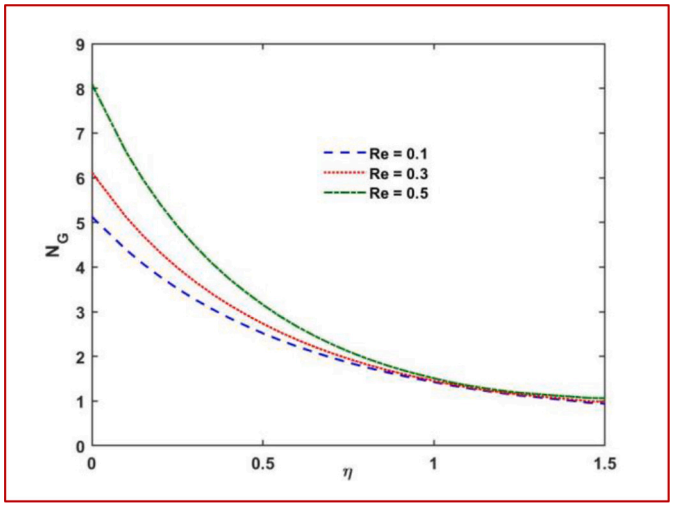

Fig. 11. $N_G(\eta)$ *versus* Re .

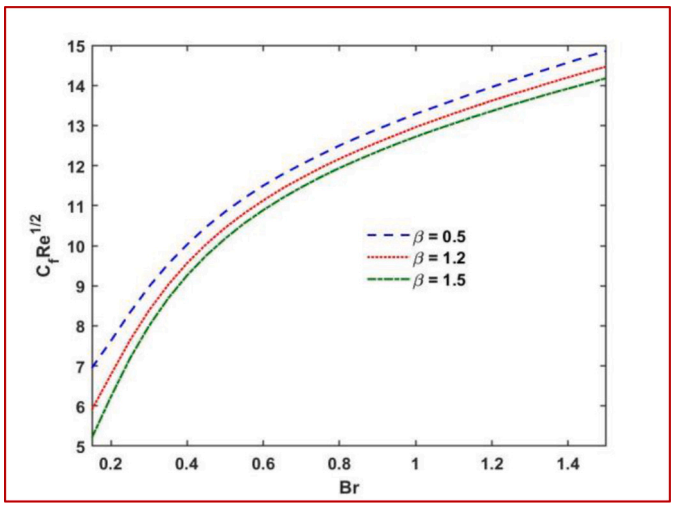

Fig. 12. *Skin friction versus Br and β.*

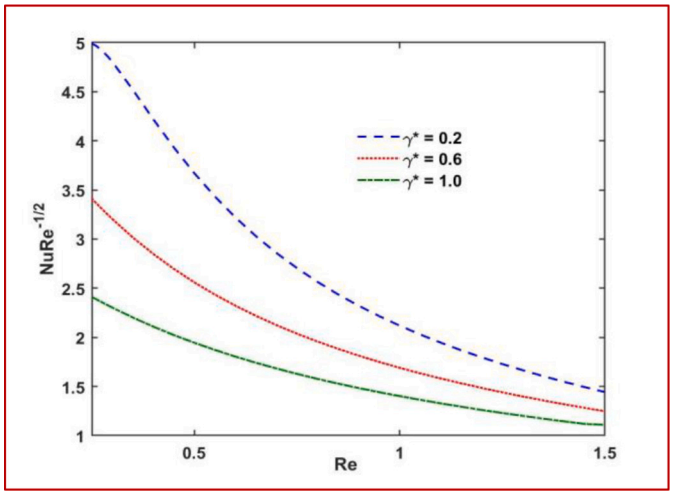

Fig. 14. *Nusselt number versus Re and γ^*.*

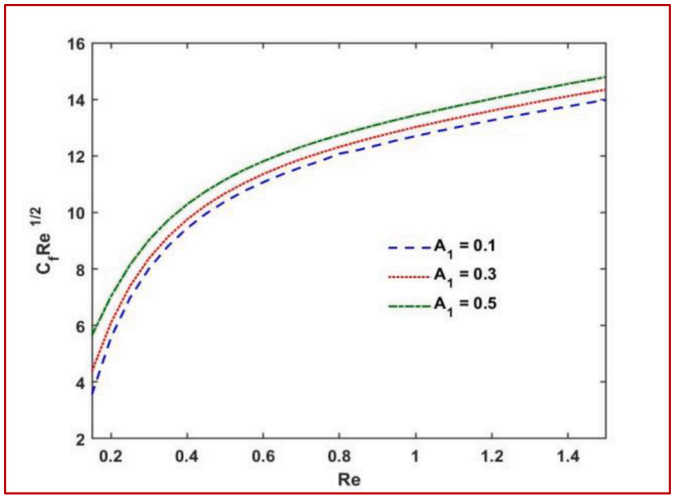

Fig. 13. *Skin friction versus Re and A_1.*

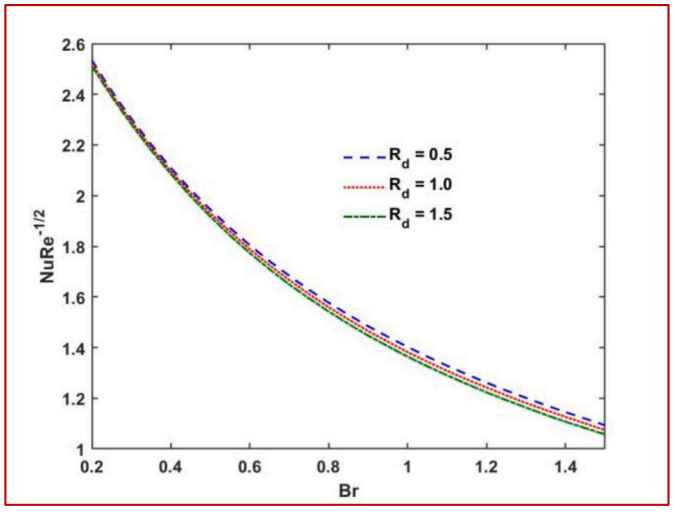

Fig. 15. *Nusselt number versus Br and R_d.*

parameter on velocity profile ($f'(\eta)$). One can detect that rising values of the porosity parameter tend to a lowering the magnitude of radial velocity field due to the presence of porous medium. Fig. 3 displays that enhancement in mixed convection parameter tends to decrement in velocity field. Fig. 4 illustrate the effect of the inertia coefficient parameter on velocity profiles ($f'(\eta)$). It is observed from this figure is that the decrement in the velocity profiles ($f'(\eta)$) for enhancing the F_r. The physical explanation, behind this reason, is that an enhancement in the F_r tends to diminishes the fluid velocity because of increasing the quadratic drag force. Variations of porosity parameter (λ), on tangential velocity profile $g(\eta)$ is shown in Fig. 5. Cleary, the tangential velocity field is lowering function of porosity parameter. The physical explanation, behind this reason is that enhancing the value of permeability of porous medium K^* which leads to decreases the friction of porous medium, so the tangential velocity $g(\eta)$ of fluid is diminishes. Fig. 6 portrays the impact of the tangential velocity slip parameter (γ) via the velocity profile $g(\eta)$. Observing that, by ascending the velocity slip parameter tends to enhancing the tangential velocity profile.

In Fig. 7 plotted the impact of temperature field $\theta(\eta)$ for distinct values of radiation parameter (R_d). Observing, the temperature profile increases for increasing the radiation parameter. Physically the thermal radiations are proportional to enhance the conversion of internal energy to the thermal energy of hybrid-nanofluids. Therefore greater the thermal energy tends to increases the temperature field. Fig. 8 shows the temperature profile diminishes against enhancing the thermal slip parameter. Physically, a small quantity of heat transfer rate to the nanofluids in the existence of thermal slip which leads to temperature field decay.

6. Analysis of entropy

In this segment, the behavior of various parameters on the entropy generation rate are analyzed through graphs. Therefore, Figs. 9-11 are portrayed the effects of sundry parameters like radiation parameters (R_d), Reynolds number (Re) and Brinkman number (Br) on entropy generation rate (N_G). Fig. 9 displays the impact of the radiation parameter (R_d) on entropy generation rate (N_G). It is noticeably that enhancing the radiation parameter leads to increasing entropy generation rate. Physically enhancing the radiation parameter tends to increment in the conversion of internal energy to the thermal energy of the system. Therefore higher the thermal energy responsible for increasing the entropy generation rate. Fig. 10 displayed that rises in Brinkman number (Br) leads to enhance the entropy generation. Fig. 11 highlight the impact of Re on entropy generation rate. From this Fig., observing that (N_G) monotonically rises against greater values of (Re). Physically, viscosity diminishes for greater values of (Re)..

7. Engineering quantities

7.1. Skin friction coefficient

The change in the behavior of the skin friction coefficient for appropriate flow parameters such as Brinkman number (Br), velocity slip parameter (β), Reynolds number (Re), and stretching parameter (A_1) is displayed in Fig. 12 and Fig. 13. The Fig. 12 shows the impact of radial velocity slip parameter (β) and Brinkman number on ($C_f\mathrm{Re}^{1/2}$). It has been observed that skin friction coefficient is monotonically rising function of Brinkman number, while decreasing function of radial velocity slip parameter. Fig. 13 portrayed the impact of skin friction coefficient for the variations of stretching parameter (A_1) versus Reynolds number (Re). It has been observed that enhancing the values of stretching parameter and Reynolds number lead to increases the coefficient of skin friction ($C_f\mathrm{Re}^{1/2}$)..

7.2. Nusselt number

In this subsection, we are examined the effects of sundry parameters such as Reynolds number (Re), thermal slip parameter (γ^*), radiation parameter (R_d) and Brinkman number (Br) via Nusselt number ($Nu\mathrm{Re}^{-1/2}$). Fig. 14 shows the impact of thermal slip parameter (γ^*) and (Re) Re against Nusselt number. It has been noticed that Nusselt number diminishes for greater values of thermal slip parameter while decreases with an enhancement in (Br). Fig. 15 displays the impact of Nusselt number for radiation parameter against Brinkman number. It has been viewed that the Nusselt number ($Nu\mathrm{Re}^{-1/2}$) decreasing for both the radiation parameter as well as Brinkman number (Br)..

8. Concluding remarks

The final remarks are given as:

- Magnitude of radial velocity $f'(\eta)$ decay versus enhancing the porosity parameter while increasing for mixed convection parameter and inertia coefficient parameter (F_r).
- Magnitude of tangential velocity profile $g(\eta)$ reduces against both porosity parameter (λ) and tangential velocity slip parameter (γ).
- An enhancement in thermal radiation parameter (R_d) leads to rises the temperature field $\theta(\eta)$ while opposite behavior has been seen for temperature slip parameter (γ^*).
- Entropy generation rate is rising function of radiation parameter (R_d) and Reynolds number (Re) and reverse trend is observed for Brinkman number (Br).

Declaration of Competing Interest

The authors declare that they have no known competing financial interests or personal relationships that could have appeared to influence the work reported in this paper.

References

[1] J.C. Maxwell, A Treatise on Electricity and Magnetism, 3rd ed., Dover Publications, New York, 1954, pp. 440–441.
[2] Q.Z. Xue, Model for thermal conductivity of carbon nanotube-based composites, Phys. B Condens. Matter 368 (2005) 302–307.
[3] X. Wang, X. Xu, S.U.S. Choi, Thermal conductivity of nanoparticle-fluid mixture, J. Thermophys. Heat Transf. 13 (1999) 474–480.
[4] T.V. Kármán, Über laminare und turbulente Reibung, J. Appl. Math. Mech. 1 (1921) 233–252.
[5] W.G. Cochran, The flow due to a rotating disc, in: Mathematical Proceedings of the Cambridge Philosophical Society 30, Cambridge University Press, 1934, pp. 365–375.
[6] E.R. Benton, On the flow due to a rotating disk, J. Fluid Mech. 24 (1966) 781–800.
[7] R. Muhammad, M.I. Khan, N.B. Khan, M. Jameel, Magnetohydrodynamics (MHD) radiated nanomaterial viscous material flow by a curved surface with second order slip and entropy generation, Comput. Methods Prog. Biomed. 189 (2020) 105294.
[8] R. Muhammad, M.I. Khan, M. Jameel, N.B. Khan, Fully developed Darcy-Forchheimer mixed convective flow over a curved surface with activation energy and entropy generation, Comput. Methods Prog. Biomed. 188 (2020) 105298.
[9] M.K. Nayak, N.S. Akbar, V.S. Pandey, Z.H. Khan, D. Tripathi, 3D free convective MHD flow of nanofluid over permeable linear stretching sheet with thermal radiation, Powder Technol. 315 (2017) 205–215.
[10] M.K. Nayak, A.K.A. Hakeem, B. Ganga, M.I. Khan, M. Waqas, O.D. Makinde, Entropy optimized MHD 3D nanomaterial of non-Newtonian fluid: a combined approach to good absorber of solar energy and intensification of heat transport, Comput. Methods Prog. Biomed. 186 (2020) 105131.
[11] T. Hayat, M.I. Khan, M. Waqas, A. Alsaedi, On the performance of heat absorption/generation and thermal stratification in mixed convective flow of an Oldroyd-B fluid, Nucl. Eng. Technol. 8 (2017) 1645–1653.
[12] S. Farooq, M.I. Khan, A. Riahi, W. Chammam, W.A. Khan, Modeling and interpretation of peristaltic transport in single and multi-walls carbon nanotubes with entropy optimization and Newtonian heating, Comput. Methods Prog. Biomed. 192 (2020) 105435.
[13] M.I. Khan, S. Qayyum, S. Kadry, W.A. Khan, S.Z. Abbas, Theoretical investigations of entropy optimization in electro-magneto nonlinear mixed convective second order slip flow, J. Magnet. 25 (2020) 8–14.
[14] M. Inc, H. Khan, D. Baleanu, A. Khan, Modified variational iteration method for straight fins with temperature dependent thermal conductivity, Therm. Sci. 22 (2018) S229–S236.
[15] A. Kilicman, Y. Khan, A. Akgül, N. Faraz, E.K. Akgül, M. Inc, Analytic approximate solutions for fluid flow in the presence of heat and mass transfer, Therm. Sci. 22 (2018) S259–S264.
[16] M. Farooq, M.I. Khan, M. Waqas, A. Alsaedi, MHD stagnation point flow of viscoelastic nanofluid with non-linear radiation effects, J. Mol. Liq. 221 (2016) 1097–1103.
[17] A. Akgül, M.S. Hashemi, M. Inc, D. Baleanu, H. Khan, New method for investigating the density-dependent diffusion nagumo equation, Therm. Sci. 22 (2018) S143–S152.
[18] M. Waqas, S. Jabeen, T. Hayat, M.I. Khan, A. Alsaedi, Modeling and analysis for magnetic dipole impact in nonlinear thermally radiating Carreau nanofluid flow subject to heat generation, J. Magn. Magn. Mater. 485 (2019) 197–204.
[19] S.R.R. Reddy, P.B.A. Reddy, K. Bhattacharyya, Effect of nonlinear thermal radiation on 3D magneto slip flow of Eyring-Powell nanofluid flow over a slendering sheet with binary chemical reaction and Arrhenius activation energy, Adv. Powder Technol. 30 (2019) 3203–3213.
[20] M.I. Khan, A. Alsaedi, S.A. Shehzad, T. Hayat, Hydromagnetic nonlinear thermally radiative nanoliquid flow with Newtonian heat and mass conditions, Results Phys. 7 (2017) 2255–2260.
[21] M. Bilal, Micropolar flow of EMHD nanofluid with nonlinear thermal radiation and slip effects, Alexandria Eng. J. 59 (2020) 965–976.
[22] M.I. Khan, M. Waqas, T. Hayat, M.I. Khan, A. Alsaedi, Melting heat transfer in stagnation point of Carreau fluid with nonlinear thermal radiation and heat source, Br. J. Mech. Sci. Eng. 40 (2018) 270.
[23] M.I. Afridi, M. Qasim, Second law analysis of Blasius flow with nonlinear Rosseland thermal radiation in the presence of viscous dissipation, Propul. Power Res. 8 (2019) 234–242.
[24] T. Hayat, M. Kanwal, S. Qayyum, M.I. Khan, A. Alsaedi, Entropy generation optimisation in the nanofluid flow of a second grade fluid with nonlinear thermal radiation, Pramana 93 (2019) 54.
[25] H. Sithole, H. Mondal, P. Sibanda, Entropy generation in a second grade magnetohydrodynamic nanofluid flow over a convectively heated stretching sheet with nonlinear thermal radiation and viscous dissipation, Results Phys. 9 (2018) 1077–1085.
[26] A. Bejan, Entropy generation through heat and fluid flow, J. Appl. Mech. 50 (1983) 475.
[27] A. Bejan, Second law analysis in heat transfer, Energy 5 (1980) 720–732.
[28] A. Arikoglu, G. Komurgoz, I. Ozkol, Effect of slip on the entropy generation from a single rotating disk, J. Fluids Eng. 10 (2008) 101202.
[29] T. Hayat, M.I. Khan, T.A. Khan, M.I. Khan, S. Ahmad, A. Alsaedi, Entropy generation in Darcy-Forchheimer bidirectional flow of water-based carbon nanotubes with convective boundary conditions, J. Mol. Liq. 265 (2018) 629–638.
[30] M. Rashid, M.I. Khan, T. Hayat, M.I. Khan, A. Alsaedi, Entropy generation in flow of ferromagnetic liquid with nonlinear radiation and slip condition, J. Mol. Liq. 276 (2019) 441–452.
[31] H. Abbasi, Entropy generation analysis in a uniformly heated microchannel heat sink, Energy 10 (2007) 1932–1947.
[32] M.I. Khan, A. Kumar, T. Hayat, M. Waqas, R. Singh, Entropy generation in flow of Carreau nanofluid, J. Mol. Liq. 278 (2019) 677–687.
[33] M.I. Khan, T. Hayat, M.I. Khan, M. Waqas, A. Alsaedi, Numerical simulation of hydromagnetic mixed convective radiative slip flow with variable fluid properties: a mathematical model for entropy generation, J. Phys. Chem. Solids 125 (2019) 153–164.

[34] G.S. Seth, R. Kumar, A. Bhattacharyya, Entropy generation of dissipative flow of carbon nanotubes in rotating frame with Darcy-Forchheimer porous medium: a numerical study, J. Mol. Liq. 268 (2018) 637–646.
[35] M.I. Khan, S. Qayyum, T. Hayat, A. Alsaedi, Entropy generation minimization and statistical declaration with probable error for skin friction coefficient and Nusselt number, Chin. J. Phys. 56 (2018) 1525–1546.
[36] L.F. Shampine, J. Kierzenka, W.M. Reichelt, Solving boundary value problems for ordinary differential equations in MATLAB with bvp4c, Tutorial Notes 2000 (2000) 1–27.
[37] M.I. Khan, M. Waqas, T. Hayat, A. Alsaedi, A comparative study of Casson fluid with homogeneous-heterogeneous reactions, J. Colloid Interface Sci. 498 (2017) 85–90.